IEICE TRANS. COMMUN., VOL.E94–B, NO.2 FEBRUARY 2011

INVITED PAPER Special Section on Extremely Advanced Optical Transmission Technologies and Transmission Optical Fiber Technologies towards Exabit Era

Ultra-Long-Haul WDM Transmission with High Spectral Efficiency

Yi CAI[†a)], **Jin-Xing CAI**[†], **Carl R. DAVIDSON**[†], **Dmitri G. FOURSA**[†], **Alan J. LUCERO**[†], **Oleg V. SINKIN**[†], **Yu SUN**[†], **Alexei N. PILIPETSKII**[†], **Georg MOHS**[†], ***and*** **Neal S. BERGANO**[†], ***Nonmembers***

SUMMARY We review our recent work on ultra-long-haul wavelength division multiplexed (WDM) transmission with high spectral efficiency (SE) employing tight pre-filtering and multi-symbol detection. We start the discussion with a theoretical evaluation of the SE limit of pre-filtered modulation in optical fiber communication systems. We show that pre-filtering induced symbol correlation generates a modulation with memory and thus, a higher SE limit than that of the original memory-less modulation. We also investigate the merits of utilizing the pre-filtering induced symbol correlation with multi-symbol detection to achieve high SE transmission. We demonstrate transoceanic WDM transmission of a pre-filtered polarization division multiplexed return-to-zero quaternary phased shift keying (PDM-RZ-QPSK) modulation format with multi-symbol detection, achieving 419% SE which is higher than the SE limit of the original memory-less PDM-RZ-QPSK format.

key words: *optical fiber communication, spectral efficiency, coherent detection, pre-filtering, MAP detection*

1. Introduction

High spectral efficiency (SE) is becoming a key requirement for further advancement in optical fiber communication systems to satisfy the increasing capacity demand. Achieving high SE is, however, particularly challenging for ultra-long-haul transmission systems such as transoceanic cable systems. Digital coherent detection techniques have enabled high SE transmission techniques such as polarization multiplexing, multi-level modulation, and orthogonal frequency division multiplexing [1]–[4]. These techniques are based on memoryless modulation formats with well defined theoretical SE limits. High SE transmission can also be achieved by employing tight pre-filtering and multi-symbol detection, which has been previously studied and demonstrated in intensity-detection systems [5]–[7]. In this paper, we investigate a high SE scheme employing pre-filtered BPSK or QPSK format together with multi-symbol based coherent detection that can yield SE exceeding the limit of memoryless QPSK modulation [8]–[11].

We start the investigation with a theoretical evaluation of the SE limit of pre-filtered modulation in optical fiber communication systems with amplified spontaneous emission (ASE) noise being the dominant impairment. We show that pre-filtering-induced symbol correlation generates a more complex modulation with memory and thus, a higher SE limit than that of the original memoryless modulation [11].

In practical implementations, however, pre-filtering induced symbol correlation causes receiver sensitivity penalty in single-symbol detection, which is commonly referred to as inter-symbol-interference (ISI) penalty. Due to the ISI penalty, a required performance that is above the forward error correction (FEC) threshold may not be achievable with single symbol detection. It requires multi-symbol waveform detection to achieve the optimal receiver sensitivity in the tightly pre-filtered case. In practical terms, a multi-symbol detection scheme such as maximum a posteriori probability (MAP) [8]–[10] or maximum likelihood sequence estimation (MLSE) [5]–[7] can help to mitigate most of the ISI penalty. In a series of transmission experiments employing the proposed pre-filtering and multi-symbol detection scheme, we demonstrate transoceanic transmission with up to 419% SE with a pre-filtered PDM-QPSK format. This SE exceeds the 400% SE limit of a memory-less PDM-QPSK modulation without symbol correlation.

The paper is organized as follows: Sect. 2 evaluates the SE limit of pre-filtered modulation for a linear optical fiber channel. Section 3 describes the high SE scheme with pre-filtering and multi-symbol detection. Section 4 reports on the experimental results demonstrating transoceanic WDM transmission with high SE. Section 5 further discusses the work comparing high SE schemes including implementation considerations and long-haul cable system evolution. Section 6 summarizes the paper and draws conclusions.

2. Spectral Efficiency Limit of Pre-Filtered Modulation for a Linear Optical Fiber Channel

The SE limit of a memory-less modulation format can be derived assuming independent transmitted symbols, which simplifies the SE limit analysis [12]–[14]. The independency condition, however, does not hold in the pre-filtered case. To evaluate the SE limit of a pre-filtered modulation format we need to take into account the pre-filtering induced symbol correlation.

Figure 1 depicts the spectrum of a binary modulation format before and after pre-filtering along with 6 representative sinc pulses [11]. Figure 1(a) shows that the original BPSK modulation occupies a bandwidth of W and all 6 pulses can be modulated independently in the time domain. Each of the 6 pulses carries 1-bit of information

Manuscript received October 18, 2010.
Manuscript revised November 19, 2010.

[†]The authors are with Tyco Electronics Subsea Communications LLC, USA.
a) E-mail: ycai@subcom.com

DOI: 10.1587/transcom.E94.B.392

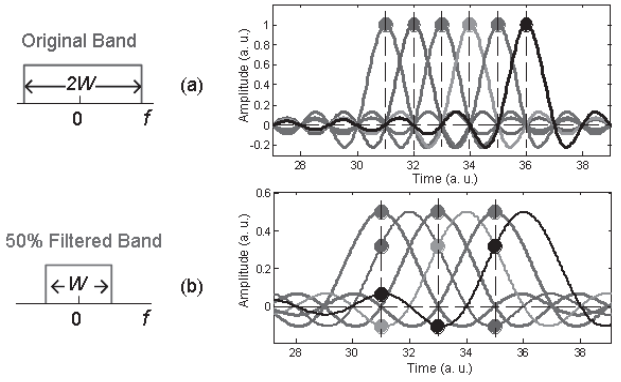

Fig. 1 Spectrum and pulses of a binary modulation (a) before and (b) after pre-filtering, where the dashed lines indicate sampling instant.

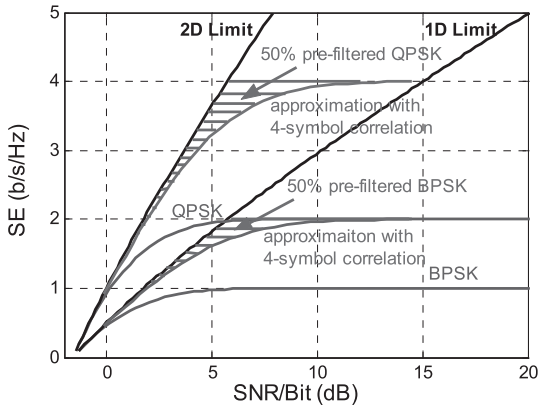

Fig. 2 Upper and lower SE bounds for 50% pre-filtered BPSK and QPSK modulation for single polarization (1D and 2D limit are for 1 dimensional and 2 dimensional modulation, respectively).

without interfering with each other. With 50% pre-filtering (i.e. half of the spectrum is low-pass filtered) as shown in Fig. 1(b), the pulses become two times wider and start to overlap. By sampling at the center of every second pulse, we also sample energy (and thus information) from neighboring pulses through symbol correlation induced by the pre-filtering. Hence, with pre-filtering we do not necessarily lose the information carried by the original signal. The information-bearing signal energy is simply redistributed.

The general formula for the SE limit of a pre-filtered modulation and thus, correlated channel inputs is given by [13]

$$\frac{C_F}{W_F} = \lim_{T\to\infty} \frac{1}{TW_F} \iint \cdots \int_{-\infty}^{\infty} f_Y(\boldsymbol{Y}) \log_2 \frac{1}{f_Y(\boldsymbol{Y})} d\boldsymbol{Y} - \log_2(2\pi eN), \quad (1)$$

where C_F/W_F represents the SE limit of the pre-filtered modulation format, T is the total signal duration, W_F is the signal bandwidth after pre-filtering, $\boldsymbol{Y} = (y_1, y_2, \ldots, y_L, \ldots)$ is the channel output vector that is the sum of the channel input vector $\boldsymbol{X} = (x_1, x_2, \ldots, x_L, \ldots)$ and the noise vector $(n_1, n_2, \ldots, n_L, \ldots)$, $f_Y(\boldsymbol{Y})$ is the joint pdf of $\boldsymbol{Y}$, and N is the average noise power. The numerical evaluation of Eq. (1) is used to obtain an exact SE limit curve; however, it is computationally complicated due to the infinite symbol correlation length induced by the pre-filtering. We therefore simplify the SE limit calculation by taking into account a finite number (L) of correlated symbols, in which case, $f_Y(\boldsymbol{Y})$ is given by:

$$f_Y(\boldsymbol{Y}) = \sum_{\forall \boldsymbol{X}_i} p(\boldsymbol{x}_i) \prod_{j=1}^{L} \frac{1}{\sqrt{2\pi N}} \exp\left[\frac{-\left(y_i - x_{ij}\right)^2}{2N}\right], \quad (2)$$

Equation (1) can then be practically evaluated for small values of L. The SE limit of a modulation format with L correlated symbols approaches that of a pre-filtered modulation format as L approaches infinity. Based on the trend observed in the statistic distribution of the Euclidean distances in signal space as L increases, we show that the SE limit of a modulation format with finite L gives a lower bound for the SE limit of pre-filtered modulation formats (infinite L) [11].

Figure 2 plots the SE bounds for 50% pre-filtered single-polarization BPSK and QPSK with the area between the lower and upper bound shaded. For comparison, Fig. 2 also shows the SE limits of memoryless BPSK and QPSK modulation. At high signal-to-noise ratio per bit (SNR/bit) the SE limit for discrete memory-less BPSK and QPSK modulation can be almost doubled using 50% pre-filtering. At low SNR/bit, pre-filtering can also significantly increase the SE limit and push it closer to the ultimate SE limit given by the Shannon limit [11].

3. High Spectral Efficiency Transmission with Pre-Filtering and Multi-Symbol Detection

In the preceding section, we showed that it is theoretically possible to significantly improve SE with tight pre-filtering. In the following, we investigate a realization of high SE WDM transmission by using pre-filtering together with multi-symbol detection.

3.1 Pre-Filtering Induced Pattern-Dependent Symbol Correlation

In WDM systems, SE is the ratio of information rate and channel spacing. Pre-filtering helps to reduce inter-channel crosstalk for tight channel spacing, but it also induces intra-channel ISI. Figure 3 shows simulated constellations of a 28 Gbaud RZ-QPSK signal with pre-filtering bandwidths of 50 GHz, 33 GHz, 28 GHz, and 25 GHz, respectively [10]. As the baud rate/pre-filtering bandwidth ratio increases, ISI becomes more severe.

The pre-filtered QPSK format can be treated as a modulation format with memory. As neighboring symbols exchange energy through ISI, they become interdependent. A closer look at the complex constellations in Fig. 3 reveals that in each of the 4 QPSK constellation groups there are 9 subgroups. This observation indicates that pre-filtering induces strong correlation between a symbol and its two nearest neighbor symbols. In Table 1, the 9 constellation subgroups are labeled as 0 to 8 in order from left to right and

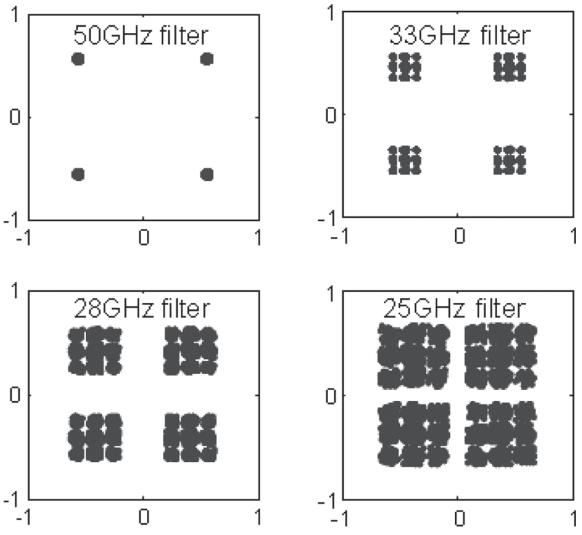

Fig. 3 Constellations of a 28 Gbaud RZ-QPSK signal at different pre-filtering bandwidths.

Table 1 Pre-filtering induced symbol correlations.

Constellation subgroup	Neighbor QPSK symbols preceding	following
0	(−1, +1)	(−1, +1)
1	(−1, +1)	(+1, +1)
	(+1, +1)	(−1, +1)
2	(+1, +1)	(+1, +1)
3	(−1, −1)	(−1, +1)
	(−1, +1)	(−1, −1)
4	(−1, −1)	(+1, +1)
	(+1, +1)	(−1, −1)
	(+1, −1)	(−1, +1)
	(−1, +1)	(+1, −1)
5	(+1, +1)	(+1, −1)
	(+1, −1)	(+1, +1)
6	(−1, −1)	(−1, −1)
7	(−1, −1)	(+1, −1)
	(+1, −1)	(−1, −1)
8	(+1, −1)	(+1, −1)

top to bottom according to their locations shown in Fig. 3. The corresponding two nearest neighbor symbols are listed in their vector format in the right column of Table 1.

Table 1 shows that a constellation subgroup can have multiple combinations of neighboring symbols due to the symmetrical nature of the pre-filtering induced symbol correlation. It also shows that these subgroups have different densities assuming equal probability of transmitted QPSK symbols. The closer a subgroup is to the center (the 4th subgroup), the higher its degeneracy.

3.2 Multi-Symbol Detection for Correlated Symbols

Since the pre-filtering induced symbol correlation is highly data-pattern dependent, it is intuitively appealing to apply a multi-symbol detection scheme to mitigate the data-pattern dependent ISI impairment. Figure 4 depicts a MAP-based multi-symbol detection scheme [8], [10].

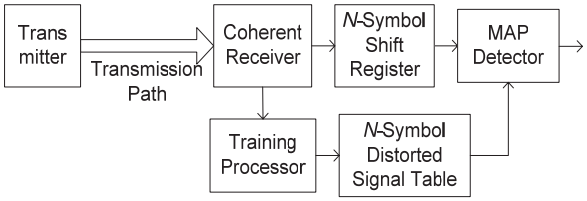

Fig. 4 A multi-symbol detection system for ISI mitigation.

A coherent receiver is employed to detect the electrical field of the received signal. A signal distortion (or ISI) table indexed by N-symbol patterns can be generated by averaging through a training sequence, or from calculations with knowledge of the system setup. Received user data in an N-symbol shifting window are fed into the MAP detector. The a posteriori probability can be calculated based on Euclidean distance or correlation between the received signal and entries in the signal-distortion table. The pattern in the table that has the shortest Euclidean distance or highest correlation to the received signal is chosen as the MAP decision.

4. Experimental Demonstration

A series of experiments were performed to investigate the performance of the proposed high SE scheme with pre-filtering and multi-symbol detection [9], [15].

4.1 Experimental Setup

Figure 5 depicts a schematic of the transmitter setup used in [9]. We electrically generate four binary 28 Gb/s signals (I, I-bar and Q, Q-bar with PRBS length $2^{23}-1$) by multiplexing 14 Gb/s data streams from a four channel pulse pattern generator (PPG). The 28 Gb/s streams are used in pairs for the I and Q ports of two QPSK modulators to generate two optical QPSK signals at 28 Gbaud or equivalently 56 Gb/s. After RZ pulse carving, each of the two optical signals is then split into two equal paths. One path is delayed with respect to the other to de-correlate the data patterns. The two data paths are then orthogonally recombined using a polarization beam combiner (PBC) resulting in two 112 Gb/s PDM RZ QPSK signals.

Each of the two QPSK modulators imparts its data onto a comb of wavelengths to generate two rails of odd and even channels. The two rails are pre-filtered and combined with cascaded 33 GHz, 28 GHz, or 25 GHz optical interleaving filters. Assuming 7% FEC overhead, the corresponding SEs are 317%, 374%, and 419%, respectively. Each rail consists of 48 DFB lasers and 4 tunable external cavity lasers (ECLs) with 1 pm resolution. The eight ECLs are tuned to a contiguous set of channels and the corresponding DFB lasers

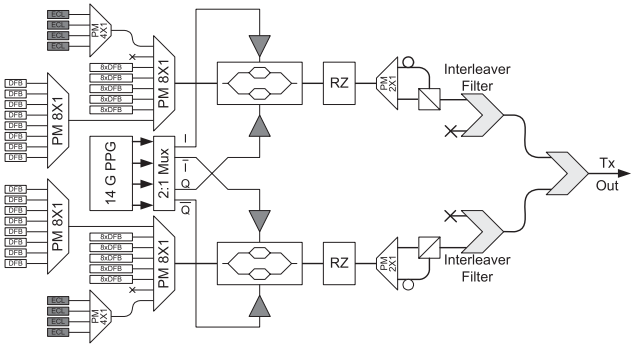

Fig. 5 112 Gb/s PDM RZ QPSK transmitter.

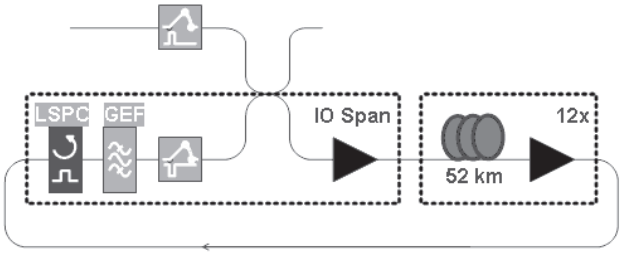

Fig. 6 Circulating loop test-bed.

are disabled for the bit error measurements. This process is repeated and the ECLs are tuned across the band until all 96 channels are measured. All 96 channels are modulated in a similar fashion at all times.

The 624 km circulating loop test-bed shown in Fig. 6 consists of twelve 52 km spans using a large effective area fiber with $A_{eff} \approx 150\,\mu m^2$, mid-band chromatic dispersion ≈ 20.6 ps/nm/km, and attenuation about 0.183 dB/km. Each span is equipped with a single-stage erbium doped fiber amplifier (EDFA) gain equalized to 26 nm bandwidth. The loop specific span contains a loop synchronous polarization controller (LSPC) [16] and a gain equalization filter to compensate residual loop gain error. The average DGD of the loop is 1.7 ps.

Figure 7 depicts the structure of the coherent receiver and function blocks in the offline digital signal processing (DSP). The coherent receiver consists of cascaded interleaver filters combined with a tunable band-pass filter to demultiplex the channel, followed by a polarization diversity 90° optical hybrid and four balanced detectors. The electrical signals from the detectors are recorded using a digital sampling scope with 16 GHz analog bandwidth and 50 GS/s sampling rate.

The recorded electrical signals are digitally processed offline. After waveform recovery and alignment, dispersion compensation is performed digitally in the Fourier domain. The resulting waveform is then re-sampled with the recovered clock. A constant modulus algorithm was used for polarization tracking and PMD compensation. Carrier phase estimation is subsequently applied using the Viterbi-Viterbi algorithm [17]. Then the multi-symbol detection is applied and decisions are made based on a MAP criterion.

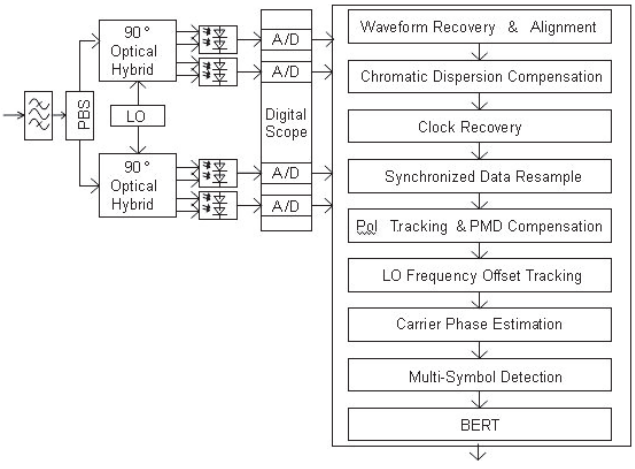

Fig. 7 Coherent receiver and DSP function blocks.

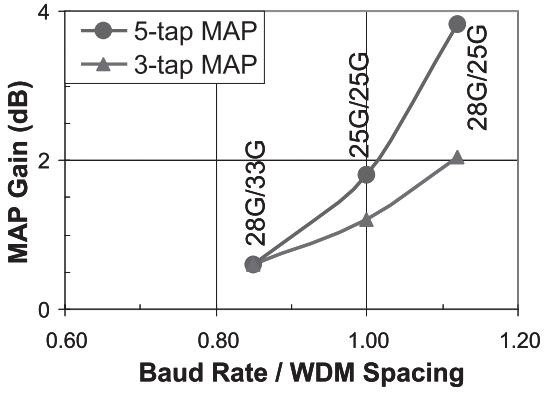

Fig. 8 Multi-symbol detection benefit at different ratio of baud rate and WDM channel spacing.

4.2 Long-Haul WDM Transmission with High Spectral Efficiency

Figure 8 shows the performance improvement achieved with MAP detection on pre-filtered 28 Gbaud and 25 Gbaud PDM-RZ-QPSK signals in back-to-back WDM experiments at baud rate/channel spacing ratios of 28/33, 25/25, and 28/25. The MAP gain represents the measured Q-factor improvement with MAP-based multi-symbol detection against the performance achieved with independent single-symbol detection. The MAP gain increases with the baud rate/channel spacing ratio due to degraded single-symbol detection performance induced by tighter pre-filtering.

Figure 8 also compares the performance of 3-tap and 5-tap MAP detection that includes 3 and 5 symbols in multi-symbol detection, respectively. It shows that at 28 Gbaud/33 GHz a 5-tap MAP does not show noticeable advantage over a 3-tap MAP. However, with 28 Gbaud/25 GHz, 5-tap MAP detection performs ~2 dB better than 3-tap MAP detection. As aforementioned, the advantage of including more neighboring symbols in MAP

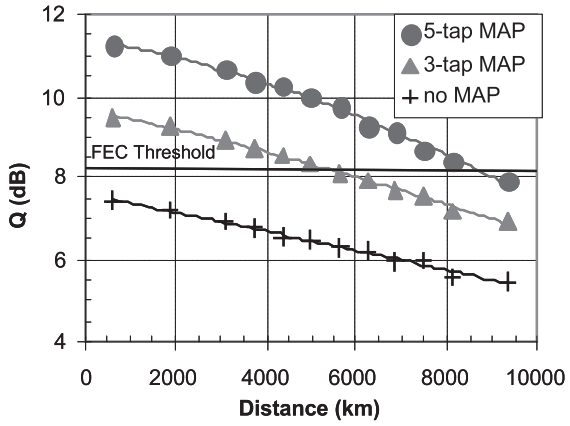

Fig. 9 419% SE WDM transmission of 28 Gbaud pre-filtered PDM RZ-QPSK signal.

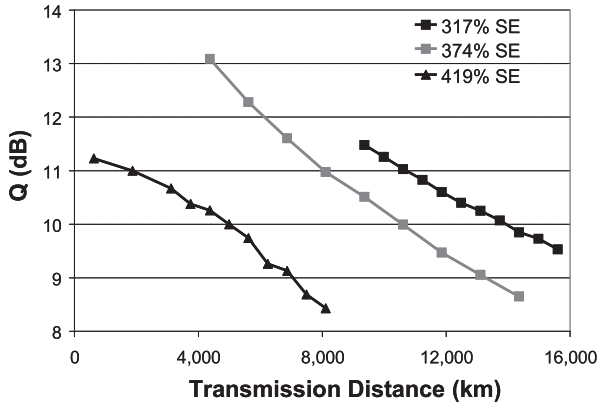

Fig. 10 WDM transmission performance of 28 Gbaud pre-filtered PDM RZ-QPSK signal vs. distance at different SEs.

detection becomes more significant at tighter pre-filtering.

Figure 9 shows the achieved Q-factor vs. distance for a channel near 1550 nm with independent single-symbol, 3-tap MAP, and 5-tap MAP detection. The 5-tap MAP detection boosted the Q-factor by ∼4 dB at 620 km and ∼2.5 dB at 9360 km. The MAP gain decreases with distance because other impairments (that cannot be mitigated by MAP detection) accumulate during transmission and become a larger portion of the overall penalty. As expected, the ISI induced by pre-filtering at 419% SE goes beyond the two immediate neighboring symbols and the 5-tap MAP outperforms the 3-tap MAP by 1–2 dB. Assuming a 7% FEC threshold of 8.2 dB, we demonstrated up to 8000 km transmission at 419% SE with 5-tap MAP detection using pre-filtered PDM RZ QPSK modulation.

Figure 10 compares the WDM transmission performance versus distance with 28 Gbaud pre-filtered PDM RZ-QPSK signal at three different SEs, i.e., 317%, 374%, and 419%, employing 5-tap MAP detection. It shows that performance and distance are significantly improved with reduction in SE from 419% to 374% and 317%. The performance difference between the 317% and 374% SE becomes larger at longer distance, which indicates that the long-haul

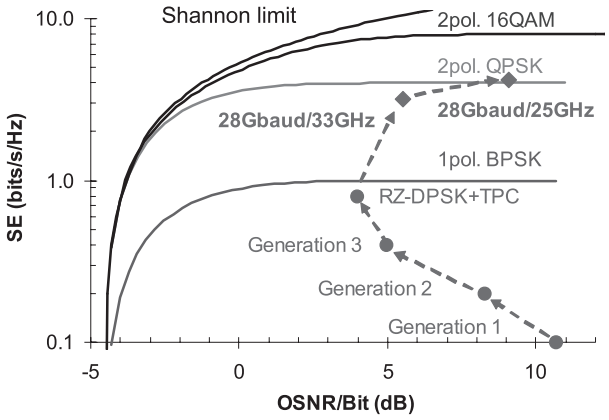

Fig. 11 Experiment results vs. SE limits, Generation 1: OOK + Reed-Solomon code, Generation 2 : OOK + concatenated Reed-Solomon code, Generation 3: DPSK + hard-decision TPC.

transmission with 374% SE is more nonlinear than that for 317% SE.

5. Discussion

The spectral efficiencies achieved in our transmission experiments are plotted in Fig. 11 for comparison with several memoryless modulation formats and previous generations of long-haul cable systems [10], [18]. The results show that the 419% SE (i.e., 28 Gbaud/25 GHz with 7% FEC) achieved with the pre-filtered PDM RZ-QPSK and multi-symbol detection exceeds the SE limit of a memoryless PDM-QPSK format, which is supported by the theoretical SE limit analysis described in Sect. 2 and originally in [11]. We also observed that the new high SE results reverse the trend of higher SE and lower required OSNR/bit achieved in previous generation systems to a trend of higher SE and higher required OSNR/bit. In previous generations, the required OSNR decreased with increasing SE as we transitioned from OOK to DPSK modulation formats and explored more advanced FEC algorithms from single Reed-Solomon codes to soft-decision turbo product code (TPC). However, as we move towards multi-level modulation formats and aggressive pre-filtering, the required OSNR increases with increasing SE as shown in Fig. 12. In our experiments we used short spans (52 km) and larger effective area fibers (150 μm^2) to enhance OSNR [9], [15].

More specifically, Fig. 12 shows the required back-to-back OSNR as a function of channel spacing with proper pre-filtering of 28 Gbaud PDM RZ-QPSK signals for 10 dB Q-factor from Monte Carlo simulation and experiment [15]. The 28 Gbaud PDM RZ-QPSK signals were pre-filtered for different channel spacings. As the channel spacing was reduced from 50 GHz to 28 GHz, the required OSNR only increased by 0.5 dB. As the channel spacing was further reduced from 28 GHz to 25 GHz, the required OSNR increased sharply by another ∼2 dB. The inflection point was ∼28 GHz in both experiment and simulation. This indicates that 28 GHz is close to the optimal channel spacing for

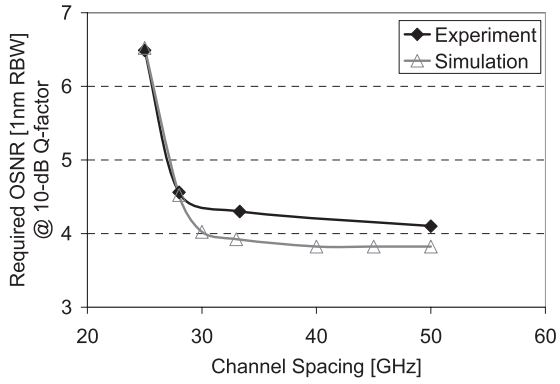

Fig. 12 Required OSNR (in 1 nm RBW) for 10 dB Q factor vs. channel spacing.

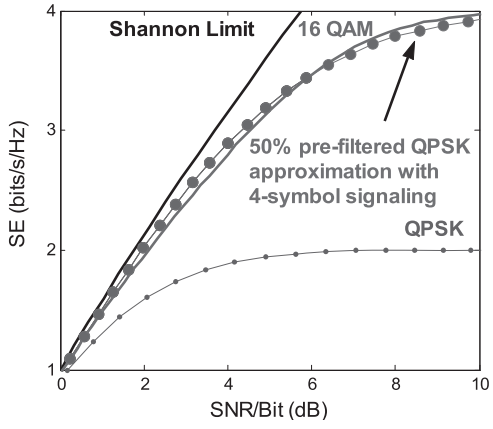

Fig. 13 SE limit comparison of 16QAM, 50% pre-filtered QPSK (lower bound of its SE limit), and regular QPSK.

28 Gbaud in terms of balancing high SE and low required OSNR, which agrees well with the results shown in [19]–[21].

Figure 13 compares the lower bound SE limit of 50% pre-filtered QPSK as derived in Sect. 2 and the actual SE limit of 16-QAM modulation [11]. It is evident that the SE limit of 16-QAM modulation is very close to the evaluated lower bound SE limit of 50% pre-filtered QPSK. The practical implementations of a memoryless 16-QAM versus a pre-filtered QPSK system, however, can be very different. To increase SE with memoryless multi-level signaling the implementation complexity on the transmitter side must be increased. On the other hand, a pre-filtered format with symbol correlation results in a more complex receiver due to the required additional algorithm that has to be implemented in the DSP of the coherent receiver for multi-symbol detection.

6. Conclusions

We investigated a high spectral efficiency transmission scheme employing tight pre-filtering and multi-symbol detection. Our theoretical analysis of the SE limit for pre-filtered modulation showed that the pre-filtering induced symbol correlation generates a modulation with memory and thus, a higher SE limit than what applies to the original memoryless modulation. We showed that the tight optical filtering introduces symbol correlation that can be utilized in the proposed multi-symbol detection scheme to mitigate the ISI penalty. We experimentally demonstrated transoceanic transmission using a pre-filtered PDM-RZ-QPSK format with MAP detection achieving 419% SE. This exceeds the 400% SE limit of the original memory-less PDM-RZ-QPSK format.

References

[1] M. Salsi, H. Mardoyan, P. Tran, C. Koebele, E. Dutisseuil, G. Charlet, and S. Bigo, "155 × 100 Gbit/s coherent PDM-QPSK transmission over 7,200 km," Proc. ECOC'09, paper PD2.5, 2009.

[2] A. Sano, H. Masuda, T. Kobayashi, M. Fujiwara, K. Horikoshi, E. Yoshida, Y. Miyamoto, M. Matsui, M. Mizoguchi, H. Yamazaki, Y. Sakamaki, and H. Ishii, "69.1-Tb/s (432 × 171-Gb/s) C- and extended L-band transmission over 240 km using PDM-16-QAM modulation and digital coherent detection," Proc. OFC/NFOEC'10, paper PDPB7, 2010.

[3] P. Winzer, A.H. Gnauck, S. Chandrasekhar, S. Draving, J. Evangelista, and B. Zhu, "Generation and 1,200-km Transmission of 448-Gb/s ETDM 56-Gbaud PDM 16-QAM using a Single I/Q Modulator," Proc. ECOC'10, paper PD2.2, 2010.

[4] X. Liu, S. Chandrasekhar, B. Zhu, P.J. Winzer, A.H. Gnauck, and D.W. Peckham, "Transmission of a 448-Gb/s reduced-guard-interval CO-OFDM signal with a 60-GHz optical bandwidth over 2000 km of ULAF and five 80-GHz-Grid ROADMs," Proc. OFC/NFOEC'10, paper PDPC2, 2010.

[5] N. Alic, G.C. Papen, R.E. Saperstein, L.B. Milstein, and Y. Fainman, "Signal statistics and maximum likelihood sequence estimation in intensity modulated fiber optic links containing a single optical preamplifier," Opt. Express, vol.13, pp.4568–4579, 2005.

[6] M. Rubsamen, P.J. Winzer, and R.-J. Essiambre, "MLSE receivers for narrow-band optical filtering," Proc. OFC/NFOEC'06, paper OWB6, 2006.

[7] N. Alic, E. Myslivets, and S. Radic, "1.0 bit/s/Hz spectral efficiency in single polarization at 2000 km with narrowly filtered intensity modulated signals," Proc. IEEE Summer Topical Meeting 2008, paper TuD3.4, 2008.

[8] Y. Cai, D. Foursa, C.R. Davidson, J.-X. Cai, O. Sinkin, M. Nissov, and A. Pilipetskii, "Experimental demonstration of coherent MAP detection for nonlinearity mitigation in long-haul transmissions," Proc. OFC/NFOEC'10, paper OTuE1, 2010.

[9] J.X. Cai, Y. Cai, C.R. Davidson, D. Foursa, A. Lucero, O. Sinkin, A. Pilipetskii, G. Mohs, and N.S. Bergano, "Transmission of 96 × 100G pre-filtered PDM-RZ-QPSK channels with 300% spectral efficiency over 10,608 km and 400% spectral efficiency over 4,368 km," Proc. OFC/NFOEC'10, paper PDPB10, 2010.

[10] Y. Cai, J.X. Cai, C.R. Davidson, D. Foursa, A. Lucero, O. Sinkin, A. Pilipetskii, G. Mohs, and N.S. Bergano, "High spectral efficiency long-Haul transmission with pre-filtering and maximum a posteriori probability detection," Proc. ECOC'2010, paper We.7.C.4, 2010.

[11] Y. Cai, J.X. Cai, A. Pilipetskii, G. Mohs, and N.S. Bergano, "Spectral efficiency limits of pre-filtered modulation formats," Opt. Express, vol.18, no.19, pp.20273–20281, 2010.

[12] T. Cover and J. Thomas, Elements of Information Theory, John Wiley & Sons, New York, 1991.

[13] R.G. Gallager, Information Theory and Reliable Communication, John Wiley & Sons, New York, 1968.

[14] J.G. Proakis, Digital Communications, 4th ed., McGraw-Hill, New York, 2001.

[15] J.X. Cai, Y. Cai, Y. Sun, C.R. Davidson, D. Foursa, A. Lucero, O.

Sinkin, A. Pilipetskii, G. Mohs, and N.S. Bergano, "112 × 112 Gb/s transmission over 9,360 km with Channel Spacing Set to the Baud Rate (360% Spectral Efficiency)," Proc. ECOC'10, paper PD2.1, 2010.

[16] Q. Yu, L.-S. Yan, S. Lee, Y. Xie, and A.E. Willner, "Loop-synchronous polarization scrambling technique for simulating polarization effects using recirculating fiber loops," J. Lightwave Technol., vol.21, no.7, p.1593, 2003.

[17] A.J. Viterbi and A.M. Viterbi, "Nonlinear estimation of PSK-modulated carrier phase with application to burst digital transmission," IEEE Trans. Inf. Theory, vol.IT-29, no.4, p.543, 1983.

[18] Y. Cai, "Coherent detection in long-haul transmission systems," OFC/NFOEC 2008, paper OTuM1, San Diego, California, 2008.

[19] A. Ellis and F. Gunning, "Spectral density enhancement using coherent WDM," PTL, vol.17, pp.504–506, 2005.

[20] S. Chandrasekhar, X. Liu, B. Zhu, and D. Peckham, "Transmission of a 1.2-Tb/s 24-carrier no-guard-interval coherent OFDM superchannel over 7200-km of ultra-large-area fiber," ECOC'09, PD2.6, 2009.

[21] G. Bosco, A. Carena, V. Curri, P. Poggiolini, E. Torrengo, and F. Forghieri, "Investigation on the robustness of a Nyquist-WDM terabit superchannel to transmitter and receiver non-idealities," ECOC'10, Tu.3.A.4, 2010.

Yi Cai received the B.S. degree in optical engineering from Beijing Institute of Technology, Beijing, China, in 1992, the M.S. degree in electrical engineering from Shanghai Institute of Technical Physics, Chinese Academy of Sciences, Shanghai, China, in 1998, and the Ph.D. degree in electrical engineering from the University of Maryland Baltimore County, Baltimore, Maryland, USA, in 2001. He joined Tyco Electronics Subsea Communications in 2001. His research focuses on the application of coherent detection, forward error correction, and advanced modulation formats in optical fiber communications.

Jin-Xing Cai received the B.S. and M.S. degrees in electronic engineering from Tsinghua University, Beijing, China, in 1988 and 1994, and the Ph.D. degree in electrical engineering from the University of Southern California, Los Angeles, CA in 1999. In 1999, he joined Tyco Electronics Subsea Communications. His is focusing on ultra long-haul transmission of high speed DWDM channels with massive system aggregate capacity.

Carl R. Davidson His biography and photograph are not available.

Dmitri G. Foursa was born in Moscow, Russia, in 1960. The Diploma degree in physics, Moscow Physical and Technical Institute, Moscow, Russia, in 1983. Research Fellow of the General Physics Institute, Moscow, Russia, Ph.D. from the above institute in 1992. His research concerns nonlinear fiber optics, lasers and amplifiers. In 1990–1991 worked as an Academic visitor at Imperial College, London, UK, concentrating on an Er-doped fiber lasers and high-repetition rate trains of solitons. In 1994–1995 Postdoctoral fellowship from S.S.T.C. at Universite Libre de Bruxelles (U.L.B.), Belgium, 1995–1999 senior research scientist, investigated experimentally and numerically dark and gray solitons and their Raman amplification in optical fibers, erbium-fiber lasers, high-bit-rate pulse shaping techniques. In 1999 he joined Tyco Electronics Subsea Communications, USA, as senior member of technical staff, working on advanced optical amplifiers and transmission issues in submarine telecommunications.

Alan J. Lucero was born on Dec. 18, 1949. He received his M.S. and Ph.D. in physics in 1989 and 1993 from the University of Connecticut. He completed a two-year postdoctoral fellowship at Bell Laboratories, Crawfordhill, NJ, in 1995, and subsequently accepted a Member of Technical Staff position at AT&T Advanced Technologies Systems, Whippany, NJ, where he concentrated on development of low power consumption EDFAs and system design. In 1997 he left to assist in the establishment of the Photonics Research and Test Center for Corning, Inc., in Somerset, NJ. He joined Tyco Electronics Subsea Communications in 2000, where his current interests include linear and nonlinear properties of high spectral efficiency transport over novel dispersion maps. Dr. Lucero is a member of Phi Beta Kappa.

Oleg V. Sinkin was born in Protvino, Russia, in 1976. He received the M.S. degree Cum Laude in Applied Physics and Mathematics from Moscow Institute of Physics and Technology, Moscow, Russia, in 1999. In 1996.1999 he has also worked as a research engineer at IRE-POLUS, Moscow (IPG Photonics) designing fiber lasers and amplifiers. In 2006, he graduated with a Ph.D. degree in Electrical Engineering from the University of Maryland Baltimore County. Oleg's graduate research was focused on developing analytical and numerical techniques to model optical fiber communications, studying nonlinear fiber propagation effects and modeling experiments. He is currently a senior member of System Modeling and Signal Processing Research at Tyco Electronics Subsea Communications. Oleg is a member of the IEEE and Photonics Society since 2001.

Yu Sun received her B.S. in optical electronic engineering from University of Electrical Science and Technology of China in 1994, and Master degree of electrical engineering from Institute of Semiconductors, Chinese Academy of Sciences in 1997. In 2003, she received Ph.D. in Photonics from University of Maryland Baltimore County (UMBC). Her research was focused on long haul high speed dispersion managed soliton systems. In 2004–2008, Dr. Sun worked as a senior optical engineer at Optium Corporation (Currently Finisar), where she concentrated on design and development of analog optical fiber transmission systems. In 2008, Dr. Sun joined Tyco Electronics Subsea Communications as senior member of technical staff, where her current interests include high spectrum efficiency submarine telecommunication systems. Dr. Sun is a senior member of IEEE.

Alexei N. Pilipetskii received M.S. degree in physics from Moscow State University in 1985. From 1985 to 1994 he worked in the General Physics Institute, Russia. He received his Ph.D. in 1990 for the research in the nonlinear fiber optics. From 1994 to 1997 he was with the UMBC, where his interest shifted to the fiber optic data transmission. Since 1997 he is with TE SubCom, where he worked on a number of research and development projects. He is currently a director of a research group with the focus on the next generation technologies for the undersea transmission systems.

Georg Mohs received his Diplom in physics from the University of Dortmund, Germany in 1993 and his M.S. and Ph.D. in Optical Sciences from the University of Arizona in 1995 and 1996, respectively. During this time and in the following 2 years as Research Associate at the University of Tokyo, Japan his interests focused on semiconductor optics and ultra-fast carrier dynamics in semiconductors. In 1998 he joined the Optical Networks Research and Development group of Siemens in Munich, Germany and began working on terrestrial optical communication systems. Dr. Mohs joint Tyco Telecommunications (now Tyco Electronics Subsea Communications, LLC) Laboratories, New Jersey, USA in 2001 as Distinguished Member of the Technical Staff. He is now Director of the Transmission Research group leading the forward looking experimental work in high capacity undersea optical communication systems.

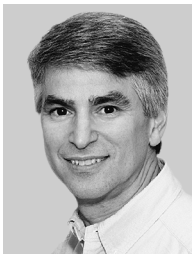

Neal S. Bergano received the B.S. degree in electrical engineering from the Polytechnic Institute of New York in 1981 and in 1983 received the M.S. degree in electrical engineering and computer science from the Massachusetts Institute of Technology, Cambridge. He is Managing Director of System Research and Network Development at Tyco Electronics Subsea Communications ("TE SubCom"). The main focus of his career has been devoted to the understanding of how to improve the performance and transmission capacity of long-haul optical fiber systems, including the use of wavelength division multiplexing in optical amplifier based systems. In 1981, he joined the technical staff of Bell Labs' undersea systems division. In 1992, he was named a Distinguished Member of the Technical Staff of AT&T Bell Labs. In 1996 he was promoted to AT&T Technology Consultant. In 1997, he was promoted to AT&T Technology Leader. Neal is on the Board of Directors for The Optical Society (OSA), and has served on the Board of Governors for IEEE LEOS from 1999 to 2001. Neal is a long-time volunteer and supporter of the OFCR/NFOEC meeting, which includes general chair and technical chair in 1999 & 1997, chair of the steering committee from 2000 to 2002, and is currently the chair of OFCR/NFOEC's long-range planning committee. Neal is a Fellow of the IEEE, OSA, AT&T and Tyco Electronics and holds 31 US patents in the area of optical fiber transmission systems. Neal S. Bergano is the recipient of the 2002 John Tyndall Award "for outstanding technical contributions to and technical leadership in the advancement of global undersea fiber optic communication systems."